

## LETTERS

# A minimum column density of $1 \text{ g cm}^{-2}$ for massive star formation

Mark R. Krumholz<sup>1,2</sup> & Christopher F. McKee<sup>3</sup>

Massive stars are very rare, but their extreme luminosities make them both the only type of young star we can observe in distant galaxies and the dominant energy sources in the Universe today. They form rarely because efficient radiative cooling keeps most star-forming gas clouds close to isothermal as they collapse, and this favours fragmentation into stars of one solar mass or lower<sup>1–3</sup>. Heating of a cloud by accreting low-mass stars within it can prevent fragmentation and allow formation of massive stars<sup>4,5</sup>, but the necessary properties for a cloud to form massive stars—and therefore where massive stars form in a galaxy—have not yet been determined. Here we show that only clouds with column densities of at least  $1 \text{ g cm}^{-2}$  can avoid fragmentation and form massive stars. This threshold, and the environmental variation of the stellar initial mass function that it implies, naturally explain the characteristic column densities associated with massive star clusters<sup>6–9</sup> and the difference between the radial profiles of H $\alpha$  and ultraviolet emission in galactic disks<sup>10,11</sup>. The existence of a threshold also implies that the initial mass function should show detectable variation with environment within the Galaxy, that the characteristic column densities of clusters containing massive stars should vary between galaxies, and that star formation rates in some galactic environments may have been systematically underestimated.

Consider a simple model system: a spherical gas cloud of mass  $M$ , column density  $\Sigma$ , radius  $R = \sqrt{[M/(\pi\Sigma)]}$ , and density profile  $\rho \propto r^{-k_p}$ , with a point source of luminosity  $L$  at its centre, representing the radiation output by stars beginning to form within it. In the limit  $L \rightarrow 0$ , the cloud falls to a background temperature  $T_b$  set by the balance between cosmic-ray heating and molecular and dust cooling. We are interested in the earliest stages of cloud collapse, so we adopt  $k_p = 1$ . This puts most of the mass at low density, and is expected if clouds are in rough hydrostatic balance and obey the observed line-width–size relation<sup>12</sup>  $\sigma \propto r^q$  for molecular clouds, where  $\sigma$  is the velocity dispersion,  $r$  is the size scale and  $q \approx 0.5$ . However, any choice in the range  $1 \leq k_p \leq 2$  yields the same qualitative conclusions.

The dust in a spherical cloud with a central source of illumination has a power-law temperature structure  $T = T_{\text{ch}}(r/R_{\text{ch}})^{-k_T}$ , where  $T_{\text{ch}}$ ,  $R_{\text{ch}}$  and  $k_T$  are functions of the cloud column density  $\Sigma$ , the light to mass ratio  $\eta \equiv L/M$ , and the dust opacity, which we characterize through a parameter  $\delta$  that we define below<sup>13</sup>. As we show in the Supplementary Information using a grain–gas energy exchange code<sup>14–16</sup>, at the high densities with which we are concerned, the gas temperature will be nearly identical to the dust temperature. The temperature will be everywhere greater than  $T_b$  if

$$T_{\text{ch}}(\eta, \Sigma, \delta) \left[ \frac{R}{R_{\text{ch}}(\eta, \Sigma, \delta)} \right]^{-k_T(\eta, \Sigma, \delta)} = T_b \quad (1)$$

Because  $k_T$  is generally close to 0.4 for strong sources of internal illumination and large  $R/R_{\text{ch}}$ , a cloud satisfying this condition has an

effective adiabatic index  $\gamma \approx 1.4$  throughout its volume. As even  $\gamma \approx 1.1–1.2$  is sufficient to suppress fragmentation<sup>5</sup>, equation (1) implicitly defines a critical light-to-mass ratio  $\eta_{\text{halt}}$  above which fragmentation will halt in a cloud with a given  $\Sigma$ ,  $\delta$  and  $T_b$ . We describe our procedure for solving this equation in the Supplementary Information.

We approximate the infrared dust opacity as  $\kappa = \delta\kappa_0(\lambda_0/\lambda)^2$ , where  $\delta$  is a dimensionless number that we define to be unity at solar metallicity,  $\lambda$  is the radiation wavelength, and  $\lambda_0 = 100 \mu\text{m}$ . Observations in the Milky Way indicate<sup>13,17</sup> that, in cold regions where dust grains are coated with ice mantles,  $\kappa_0 \approx 0.54 \text{ cm}^2 \text{ g}^{-1}$ . Under Milky Way conditions the minimum temperature for interstellar gas is  $T_b \approx 10 \text{ K}$ , with a weak density dependence that we ignore for simplicity. In addition to the Milky Way case, we also consider  $\delta = 0.25$ ,  $T_b = 10 \text{ K}$ , appropriate for a low-metallicity galaxy today, and  $\delta = 0.25$ ,  $T_b = 15 \text{ K}$ , typical of a galaxy at  $z \approx 6$  that has low metallicity but a temperature floor of 15 K imposed by the cosmic microwave background. Figure 1 shows the value of  $\eta_{\text{halt}}$  calculated for the three cases. We find that  $\eta_{\text{halt}}$  declines with  $\Sigma$  because at higher  $\Sigma$  a cloud of fixed mass has a smaller radiating area and remains warmer at fixed luminosity.

Clouds containing massive stars can have light-to-mass ratios of  $100L_{\odot}/M_{\odot}$  (ref. 18), more than sufficient to stop fragmentation, but we are interested in clouds where no massive stars have yet formed because fragmentation breaks all collapsing objects down to small masses. For a low-mass protostar the dominant energy source is gravitational potential energy radiated away by accreting gas. We plot the energy released per unit mass accreted,  $\psi$ , in Fig. 2. Consider a cloud converting its mass into stars at a rate  $\dot{M}_*$  with a mass distribution  $dn/d \ln m_*$  and a mean mass  $\bar{m}_* = \int m_* (dn/d \ln m_*) d \ln m_*$ . Once the rate at which new stars in a cloud begin accreting balances the rate at which other stars reach their final mass and stop accreting, the light-to-mass ratio is

$$\eta_{\text{grav}} = \frac{1}{M} \left( \frac{\dot{M}_*}{\bar{m}_*} \right) \int \frac{dn}{d \ln m_*} \psi m_* d \ln m_* \quad (2)$$

$$= \frac{\text{SFR}_{\text{ff}}}{\bar{t}_{\text{ff}}} \langle \psi \rangle_{\text{IMF}} \quad (3)$$

where  $\text{SFR}_{\text{ff}} = (\dot{M}_* \bar{t}_{\text{ff}})/M$  is the fraction of a cloud's mass that it turns into stars per mean density free-fall time  $\bar{t}_{\text{ff}}$ , and  $\langle \psi \rangle_{\text{IMF}} = \bar{m}_*^{-1} \int (dn/d \ln m_*) \psi m_* d \ln m_*$  is the value of  $\psi$  averaged over the initial mass function (IMF). For a Chabrier IMF<sup>19</sup> truncated at a maximum mass of  $1M_{\odot}$ ,  $\langle \psi \rangle_{\text{IMF}} = 2.1 \times 10^{14} \text{ erg g}^{-1} = 0.11 (GM_{\odot}/R_{\odot})$ . Observations constrain  $\text{SFR}_{\text{ff}}$  to be a few per cent<sup>20,21</sup>, and in the Supplementary Information we use an analytic fitting formula<sup>22</sup> to estimate  $\text{SFR}_{\text{ff}} \approx 0.041 \left( M_2 \Sigma_0 / T_{b,1}^2 \right)^{-0.08}$ , where  $M_2 = M/(100M_{\odot})$ ,  $\Sigma_0 =$

<sup>1</sup>Astrophysics Department, Princeton University, Princeton, New Jersey 08544, USA. <sup>2</sup>Astrophysics Department, University of California Santa Cruz, Santa Cruz, California 95064, USA. <sup>3</sup>Physics and Astronomy Departments, University of California Berkeley, Berkeley, California 94720, USA.

$\Sigma/(1 \text{ g cm}^{-2})$ , and  $T_{b,1} = T_b/(10 \text{ K})$ . Combining our estimates for  $\langle \psi \rangle_{\text{IMF}}$  and  $\text{SFR}_{\text{ff}}$  with the definition of the mean density free-fall time ( $\bar{t}_{\text{ff}} = \sqrt{3\pi/(32G\bar{\rho})} = 38.6M_2^{1/4}\Sigma_0^{-3/4}\text{kyr}$ ), we find that the light-to-mass ratio of a cloud powered by accretion onto low-mass stars is

$$\eta_{\text{grav}} \approx 3.6M_2^{-0.33}\Sigma_0^{0.67}T_{b,1}^{0.16}\left(\frac{L_\odot}{M_\odot}\right) \quad (4)$$

For the models shown in Fig. 2 a cloud reaches its equilibrium light-to-mass ratio within about  $3\bar{t}_{\text{ff}}$  after star formation begins, and because  $\text{SFR}_{\text{ff}}$  is less than about 0.05, at most  $\sim 15\%$  of the mass will have gone into low-mass stars at this point. If star formation accelerates in time, as predicted by some models<sup>23</sup>, then  $\eta_{\text{grav}}$  will reach the value given by equation (4) even earlier.

In Fig. 1, we show  $\eta_{\text{grav}}$  computed for some typical parameters overplotted with  $\eta_{\text{halt}}$ . For each cloud mass  $M$ , we solve equations (1) and (4) to find the column density  $\Sigma_{\text{th}}$  such that  $\eta_{\text{halt}} \geq \eta_{\text{grav}}$ , and plot the result in Fig. 3. This is the threshold required for fragmentation to halt. We find that thresholds of  $0.7\text{--}1.5 \text{ g cm}^{-2}$  are required to form stars of  $10\text{--}200M_\odot$  under Milky Way conditions. Lower-metallicity galaxies ( $0.25$  solar metallicity) with comparable background temperatures require column densities that are about a factor of 3 smaller, whereas galaxies at  $z \approx 6$  with  $0.25$  solar metallicity but high cosmic microwave background temperatures require higher column densities by a similar factor.

The existence of a threshold for massive star formation both explains current observations and predicts future ones. Regions with column densities above about  $1 \text{ g cm}^{-2}$  are rare even among star-forming clouds, and contain only a small fraction of the molecular mass in the Galaxy, but our threshold explains why all nearby regions

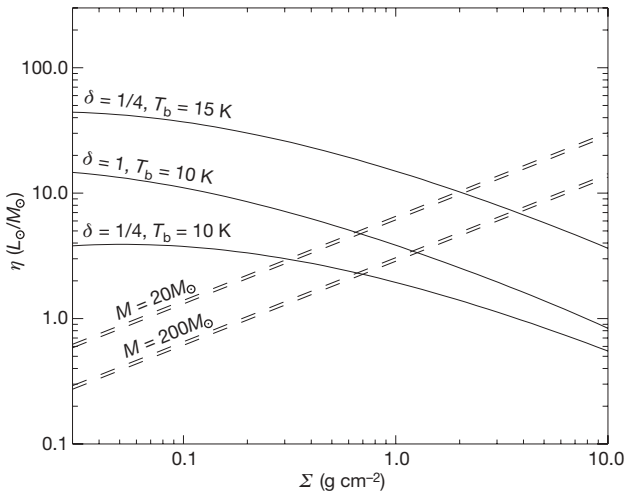


**Figure 1 | Critical and equilibrium light-to-mass ratios versus cloud column density.** The plot shows the critical light-to-mass ratio  $\eta_{\text{halt}}$  (solid lines) and the equilibrium light-to-mass ratio  $\eta_{\text{grav}}$  due to low-mass star formation (dashed lines) as a function of the cloud column density  $\Sigma$ . The three curves for  $\eta_{\text{halt}}$  are computed for  $\delta = 1$ ,  $T_b = 10 \text{ K}$ , for  $\delta = 1/4$ ,  $T_b = 10 \text{ K}$ , and for  $\delta = 1/4$ ,  $T_b = 15 \text{ K}$ , as indicated. The two sets of curves for  $\eta_{\text{grav}}$  are computed for  $M = 20M_\odot$  and  $M = 200M_\odot$ , as indicated, corresponding to the clouds that would be required to form  $10M_\odot$  and  $100M_\odot$  stars for a typical star-formation efficiency<sup>27</sup> of 50%. In each pair the lower curve corresponds to  $T_b = 10 \text{ K}$  and the upper to  $T_b = 15 \text{ K}$ . Note that the background temperature can be higher than our assumed  $T_b$  in regions near massive stars, but it is unclear whether massive stars in a cluster ever form close enough in time that the first to form can affect the formation of subsequent ones. In the Orion Nebula<sup>28</sup> and W3 Main<sup>29</sup> clusters, all the stars larger than  $10M_\odot$  that remain today formed over a time spread of less than about  $10^5 \text{ yr}$ . This is comparable to the formation time of a single massive star<sup>30</sup>, so that the last massive star to form must have been well in progress by the time the first began to heat its envelope. Even in non-coeval clusters, our approach applies to the first massive stars.

of massive star formation have  $\Sigma$  at or above this value<sup>6–9</sup>. We further predict that clusters formed with  $\Sigma \ll 1 \text{ g cm}^{-2}$  should be deficient in massive stars. This is probably unobservable in individual low- $\Sigma$  clusters because they contain too few stars, but a statistical analysis of many clusters might reveal the effect.

Conversely, suppression of fragmentation should produce top-heavy IMFs at high gas column densities. This prediction can be tested by X-ray searches for low-mass protostars in high- $\Sigma$  clouds that are not detected by Spitzer at  $24 \mu\text{m}$  and therefore contain no massive protostars<sup>24</sup>. We predict that any low-mass protostellar populations detected will constitute at most 15% of the total mass. This prediction provides a sharp test for distinguishing our model from competitive accretion models, which predict that the mass of the most massive star forming in a cloud is related to the mass of low-mass stars around it by  $(M_{\text{mass}}/M_\odot) \approx (M_{\text{low-mass}}/M_\odot)^{2/3}$  (ref. 23). Thus we would predict that a cloud of mass  $100M_\odot$  and  $\Sigma > 1 \text{ g cm}^{-2}$  with no stars larger than  $10M_\odot$  should have a total stellar content below  $15M_\odot$ , whereas competitive accretion would allow up to  $42M_\odot$  of low-mass stars. However, because radiation does not halt fragmentation until some low-mass stars have formed, we do expect most massive stars to form surrounded by a cluster.

Environmental variation at the top end of the IMF has even more profound consequences for extragalactic astronomy, as observations of distant galaxies are generally sensitive only to massive stars. The threshold explains why  $\text{H}\alpha$  emission in galactic disks ends at sharp edges where the disks transition from gravitationally unstable to gravitationally stable<sup>10</sup>, but ultraviolet emission declines smoothly with radius and does not show a feature at the  $\text{H}\alpha$  edge<sup>11</sup>. Ultraviolet and

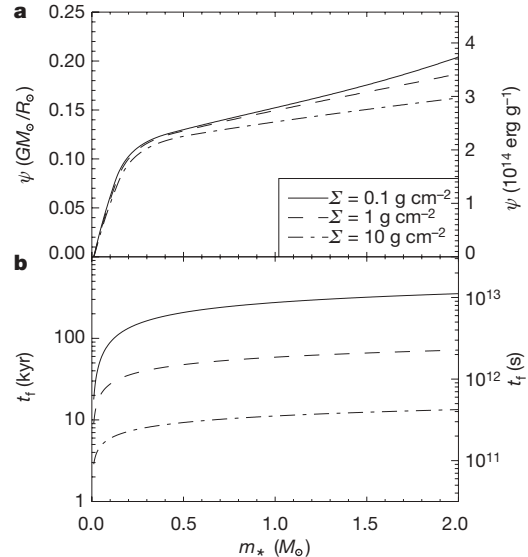


**Figure 2 | Energy per unit mass radiated and formation time versus protostellar mass.** **a**, The energy per unit mass,  $\psi$ , radiated away in the process of forming a star of mass  $m_*$ ; **b**, the time required to form the star,  $t_f$ . The tracks shown are computed using a one-zone protostellar evolution code<sup>9</sup> applied to the accretion histories predicted previously<sup>9,30</sup> using their fiducial parameters, for protostellar cores born in environments where the column density is  $\Sigma = 0.1, 1.0$  or  $10.0 \text{ g cm}^{-2}$  as indicated. However, alternative accretion histories give qualitatively identical results. Note that  $\psi$  is nearly independent of both accretion history and final stellar mass because the entropy distribution within a protostar and the protostellar mass–radius relation are nearly constant on timescales that are short compared with the Kelvin–Helmholtz time  $t_{\text{KH}}$ , and for low-mass stars  $t_f \ll t_{\text{KH}} \approx 10 \text{ Myr}$ . This means that  $\psi$ , which is a measure of the gravitational energy released, is nearly independent of accretion history. Moreover, because low-mass stars have nearly linear mass–radius relations,  $\psi$  is also nearly independent of the final stellar mass. Although our calculation of  $\psi$  uses a code calibrated to solar metallicity, our results should also apply over a very wide range of metallicities because even for low-metallicity stars  $t_f \ll t_{\text{KH}}$ .

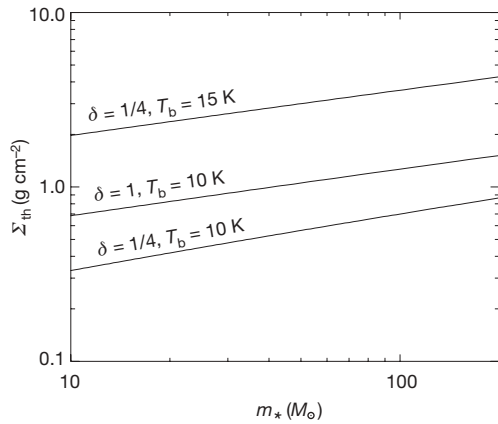


**Figure 3 | Threshold column density versus stellar mass.** The plot shows the threshold column density  $\Sigma_{\text{th}}$  required to form a star of mass  $m_*$  for  $\delta = 1$ ,  $T_b = 10$  K, for  $\delta = 1/4$ ,  $T_b = 10$  K, and for  $\delta = 1/4$ ,  $T_b = 15$  K, as indicated. In making the plot we assumed an efficiency of 50% (ref. 27), so that the cloud mass required to make a star of mass  $m_*$  is  $M = 2m_*$ .

H $\alpha$  emission are both tracers of recent star formation but are sensitive to different parts of the IMF. Outside the gravitational stability radius, the molecular-to-atomic surface density ratio drops sharply<sup>25</sup>, probably because purely local instabilities create small molecular clouds but not giant complexes like those in the inner parts of disks. Because compressing gas to column densities of  $\Sigma_{\text{th}}$  requires a huge amount of weight that can only be provided by such giant complexes, their absence will selectively suppress the formation of the most massive stars, leading to a truncated IMF. If in such a region no stars larger than, for example,  $15M_{\odot}$  were to form, this would reduce ultraviolet emission by  $\sim 50\%$  but would eliminate more than 99% of the H $\alpha$  light<sup>26</sup>, explaining the sharp drop in H $\alpha$  but not in the ultraviolet.

An important corollary is that estimates of the star formation rate assuming a standard IMF in regions that do not contain giant clouds (such as much of the volume of dwarf galaxies and the outer parts of disk galaxies) may be systematically too low. At this point our theory is too approximate to allow a precise calculation of the underestimate.

Our calculation of  $\Sigma_{\text{th}}$  also enables us to predict how the characteristic column densities of young clusters containing massive stars will vary between galaxies. We predict that clusters that have cleared their gas but not yet dynamically expanded should show a minimum column density near  $\Sigma_{\text{th}}$  (probably slightly below  $\Sigma_{\text{th}}$ , owing to gas removal), and this should be lower at low metallicity and higher at high redshift, as indicated in Fig. 3.

Received 17 October; accepted 20 December 2007.

- Larson, R. B. Thermal physics, cloud geometry and the stellar initial mass function. *Mon. Not. R. Astron. Soc.* **359**, 211–222 (2005).
- Jappsen, A.-K., Klessen, R. S., Larson, R. B., Li, Y. & Mac Low, M.-M. The stellar mass spectrum from non-isothermal gravoturbulent fragmentation. *Astron. Astrophys.* **435**, 611–623 (2005).
- Bonnell, I. A., Clarke, C. J. & Bate, M. R. The Jeans mass and the origin of the knee in the IMF. *Mon. Not. R. Astron. Soc.* **368**, 1296–1300 (2006).
- Krumholz, M. R. Radiation feedback and fragmentation in massive protostellar cores. *Astrophys. J.* **641**, L45–L48 (2006).
- Krumholz, M. R., Klein, R. I. & McKee, C. F. Radiation-hydrodynamic simulations of collapse and fragmentation in massive protostellar cores. *Astrophys. J.* **656**, 959–979 (2007).

- Plume, R., Jaffe, D. T., Evans, N. J., Martin-Pintado, J. & Gomez-Gonzalez, J. Dense gas and star formation: Characteristics of cloud cores associated with water masers. *Astrophys. J.* **476**, 730–749 (1997).
- Mueller, K. E., Shirley, Y. L., Evans, N. J. & Jacobson, H. R. The physical conditions for massive star formation: Dust continuum maps and modeling. *Astrophys. J. Suppl. Ser.* **143**, 469–497 (2002).
- Shirley, Y. L., Evans, N. J., Young, K. E., Knez, C. & Jaffe, D. T. A CS J = 5 $\rightarrow$ 4 mapping survey toward high-mass star-forming cores associated with water masers. *Astrophys. J. Suppl. Ser.* **149**, 375–403 (2003).
- McKee, C. F. & Tan, J. C. The formation of massive stars from turbulent cores. *Astrophys. J.* **585**, 850–871 (2003).
- Martin, C. L. & Kennicutt, R. C. Star formation thresholds in galactic disks. *Astrophys. J.* **555**, 301–321 (2001).
- Boissier, S. *et al.* Radial variation of attenuation and star formation in the largest late-type disks observed with GALEX. *Astrophys. J. Suppl. Ser.* **173**, 524–537 (2007).
- Heyer, M. H. & Brunt, C. M. The universality of turbulence in galactic molecular clouds. *Astrophys. J.* **615**, L45–L48 (2004).
- Chakrabarti, S. & McKee, C. F. Far-infrared SEDs of embedded protostars and dusty galaxies. I. Theory for spherical sources. *Astrophys. J.* **631**, 792–808 (2005).
- Neufeld, D. A., Lepp, S. & Melnick, G. J. Thermal balance in dense molecular clouds: Radiative cooling rates and emission-line luminosities. *Astrophys. J. Suppl. Ser.* **100**, 132–147 (1995).
- Young, K. E., Lee, J.-E., Evans, N. J. II, Goldsmith, P. F. & Doty, S. D. Probing pre-protostellar cores with formaldehyde. *Astrophys. J.* **614**, 252–266 (2004).
- Urban, A., Evans, N. J. II & Doty, S. D. A parameter study of the dust and gas temperature in a field of young stars. *Astrophys. J.* (submitted); preprint at (<http://arXiv.org/abs/0710.3906>) (2007).
- Weingartner, J. C. & Draine, B. T. Dust grain-size distributions and extinction in the Milky Way, Large Magellanic Cloud, and Small Magellanic Cloud. *Astrophys. J.* **548**, 296–309 (2001).
- Wu, J. *et al.* Connecting dense gas tracers of star formation in our galaxy to high-Z star formation. *Astrophys. J.* **635**, L173–L176 (2005).
- Chabrier, G. in *The Initial Mass Function 50 Years Later* (ed. Corbelli, E., Palla, F. & Zinnecker, H.) 41–50 (Springer, Dordrecht, 2005).
- Tan, J. C., Krumholz, M. R. & McKee, C. F. Equilibrium star cluster formation. *Astrophys. J.* **641**, L121–L124 (2006).
- Krumholz, M. R. & Tan, J. C. Slow star formation in dense gas: Evidence and implications. *Astrophys. J.* **654**, 304–315 (2007).
- Krumholz, M. R. & McKee, C. F. A general theory of turbulence-regulated star formation, from spirals to ultraluminous infrared galaxies. *Astrophys. J.* **630**, 250–268 (2005).
- Bonnell, I. A., Vine, S. G. & Bate, M. R. Massive star formation: nurture, not nature. *Mon. Not. R. Astron. Soc.* **349**, 735–741 (2004).
- Motte, F. *et al.* The earliest phases of high-mass star formation: a 3 square degree millimeter continuum mapping of Cygnus X. *Astron. Astrophys.* **476**, 1243–1260 (2007).
- Braine, J., Ferguson, A. M. N., Bertoldi, F. & Wilson, C. D. The detection of molecular gas in the outskirts of NGC 6946. *Astrophys. J.* **669**, L73–L76 (2007).
- Parravano, A., Hollenbach, D. J. & McKee, C. F. Time dependence of the ultraviolet radiation field in the local interstellar medium. *Astrophys. J.* **584**, 797–817 (2003).
- Matzner, C. D. & McKee, C. F. Efficiencies of low-mass star and star cluster formation. *Astrophys. J.* **545**, 364–378 (2000).
- Huff, E. M. & Stahler, S. W. Star formation in space and time: The Orion Nebula Cluster. *Astrophys. J.* **644**, 355–363 (2006).
- Feigelson, E. D. & Townsley, L. K. The diverse stellar populations of the W3 star forming complex. *Astrophys. J.* **673**, 354–362 (2008); preprint at (<http://arXiv.org/abs/0710.0090>) (2007).
- McKee, C. F. & Tan, J. C. Massive star formation in 100,000 years from turbulent and pressurized molecular clouds. *Nature* **416**, 59–61 (2002).

Supplementary Information is linked to the online version of the paper at [www.nature.com/nature](http://www.nature.com/nature).

**Acknowledgements** We acknowledge S. Boissier, I. Bonnell, B. Elmegreen, E. Feigelson and C. Martin for discussions. We thank A. Urban, N. Evans and S. Doty for providing a copy of their grain–gas coupling code. This work was supported by NASA through the Hubble Fellowship program and by the NSF. Parts of this work were performed while the authors were in residence at the Kavli Institute for Theoretical Physics at UCSB.

**Author Information** Reprints and permissions information is available at [www.nature.com/reprints](http://www.nature.com/reprints). Correspondence and requests for materials should be addressed to M.R.K. ([krumholz@astro.princeton.edu](mailto:krumholz@astro.princeton.edu)).